

Journal Pre-proof



LT β R Signaling Directly Controls Airway Smooth Muscle Deregulation and Asthmatic Lung Dysfunction

Haruka Miki, MD PhD, William B. Kiosses, PhD, Mario C. Manresa, PhD, Rinkesh K. Gupta, PhD, Gurupreet S. Sethi, PhD, Rana Herro, PhD, Ricardo Da Silva Antunes, PhD, Paramita Dutta, BSc, Marina Miller, MD PhD, Kai Fung, MSc, Ashu Chawla, BSc, Katarzyna Dobaczewska, BSc, Ferhat Ay, PhD, David H. Broide, MB ChB, Alexei V. Tumanov, PhD, Michael Croft, PhD

PII: S0091-6749(22)01622-0

DOI: <https://doi.org/10.1016/j.jaci.2022.11.016>

Reference: YMAI 15777

To appear in: *Journal of Allergy and Clinical Immunology*

Received Date: 23 May 2022

Revised Date: 25 October 2022

Accepted Date: 18 November 2022

Please cite this article as: Miki H, Kiosses WB, Manresa MC, Gupta RK, Sethi GS, Herro R, Da Silva Antunes R, Dutta P, Miller M, Fung K, Chawla A, Dobaczewska K, Ay F, Broide DH, Tumanov AV, Croft M, LT β R Signaling Directly Controls Airway Smooth Muscle Deregulation and Asthmatic Lung Dysfunction, *Journal of Allergy and Clinical Immunology* (2023), doi: <https://doi.org/10.1016/j.jaci.2022.11.016>.

This is a PDF file of an article that has undergone enhancements after acceptance, such as the addition of a cover page and metadata, and formatting for readability, but it is not yet the definitive version of record. This version will undergo additional copyediting, typesetting and review before it is published in its final form, but we are providing this version to give early visibility of the article. Please note that, during the production process, errors may be discovered which could affect the content, and all legal disclaimers that apply to the journal pertain.

© 2022 Published by Elsevier Inc. on behalf of the American Academy of Allergy, Asthma & Immunology.

LT β R Signaling Directly Controls Airway Smooth Muscle Deregulation and Asthmatic Lung Dysfunction

Authors:

Haruka Miki, MD PhD^{1,6}, William B. Kiosses, PhD², Mario C. Manresa, PhD¹, Rinkesh K. Gupta,
PhD¹, Gurupreet S Sethi, PhD¹, Rana Herro, PhD^{1,7}, Ricardo Da Silva Antunes, PhD¹, Paramita
Dutta, BSc¹, Marina Miller, MD PhD⁵, Kai Fung, MSc³, Ashu Chawla, BSc³, Katarzyna
Dobaczewska, BSc², Ferhat Ay, PhD¹, David H. Broide, MB ChB⁵, Alexei V Tumanov, PhD⁴,
and Michael Croft, PhD^{*1,5}

¹Center for Autoimmunity and Inflammation, ²Microscopy Core, ³Bioinformatics Core, La Jolla
Institute for Immunology, La Jolla, CA 92037, United States

⁴Department of Microbiology, Immunology and Molecular Genetics, University of Texas Health
Science Center San Antonio, San Antonio, TX, 78229, United States.

⁵Department of Medicine, University of California San Diego, San Diego, CA, 92161, United
States.

⁶Present address: University of Tsukuba, Tsukuba, Ibaraki 305-8575, Japan.

⁷Present address: Cincinnati Children's Hospital Medical Center, Immunobiology Division,
University of Cincinnati, Cincinnati OH 45229, United States

*Corresponding author: mick@lji.org

Conflict of interest statement: M.C has patents related to LIGHT and lung inflammation.

24 **ABSTRACT**

25 **Background:** Dysregulation of airway smooth muscle cells (ASM) is central to the severity of
26 asthma. Which molecules dominantly control ASM in asthmatics is unclear. High levels of the
27 cytokine LIGHT (TNFSF14) have been linked to asthma severity and lower baseline
28 FEV₁ %predicted, implying signals through its receptors might directly control ASM dysfunction.

29 **Objective:** To determine whether signaling via LTβR or HVEM from LIGHT dominantly drives
30 ASM hyperreactivity induced by allergen.

31 **Methods:** Conditional knockout mice deficient for LTβR or HVEM in smooth muscle cells were
32 used to determine their role in ASM deregulation and airway hyperresponsiveness (AHR) *in vivo*.
33 Human ASM were used to study signals induced by LTβR.

34 **Results:** LTβR was strongly expressed in ASM from normal and asthmatic subjects compared to
35 several other receptors implicated in smooth muscle deregulation. Correspondingly, conditional
36 deletion of LTβR only in smooth muscle cells in smMHC^{Cre}LTβR^{fl/fl} mice minimized changes in
37 their numbers and mass, and AHR, induced by house dust mite allergen in a model of severe
38 asthma. Intratracheal LIGHT administration independently induced ASM hypertrophy and AHR *in*
39 *vivo* dependent on direct LTβR signals to ASM. LIGHT promoted contractility, hypertrophy, and
40 hyperplasia of human ASM *in vitro*. Distinguishing LTβR from the receptors for IL-13, TNF, and
41 IL-17 that have also been implicated in smooth muscle dysregulation, LIGHT promoted NIK-
42 dependent non-canonical NF-κB in ASM *in vitro*, leading to sustained accumulation of F-actin,
43 phosphorylation of myosin light chain kinase, and contractile activity.

44 **Conclusion:** LTβR signals directly and dominantly drive airway smooth muscle
45 hyperresponsiveness relevant for pathogenesis of airway remodeling in severe asthma.

46

47 Key Messages:

- 48 • $LT\beta R$ interactions on smooth muscle cells in vivo control airway smooth muscle mass and
49 airway hyperresponsiveness driven by inhaled allergen
- 50 • LIGHT- $LT\beta R$ non-canonical NF- κB signaling promotes contractile activity, hyperplasia
51 and hypertrophy in airway smooth muscle cells

52

53 Capsule Summary:

54 Deletion of $LT\beta R$ in smooth muscle cells limits allergen-driven airway smooth muscle remodeling
55 and airway hyperresponsiveness, implying that $LT\beta R$ may control excessive bronchial smooth
56 muscle activity related to remodeling and lung function impairment in asthma.

57

58 Keywords

59 $LT\beta R$, Asthma, Airway Smooth Muscle, AHR, contractility, non-canonical NF- κB , TNF superfamily,
60 LIGHT, TNFSF14

61

62 Abbreviations

63 HDM, house dust mite; ASM, airway smooth muscle cells; AHR, airway hyperresponsiveness;
64 LIGHT, homologous to lymphotoxin, exhibits inducible expression and competes with HSV
65 glycoprotein D for binding to HVEM, a receptor expressed on T lymphocytes; HVEM, herpes virus
66 entry mediator; $LT\beta R$, lymphotoxin beta receptor; $LT\alpha\beta$, lymphotoxin alpha beta

67 INTRODUCTION

68 The pathological features of asthma are chronic airway inflammation, associated with an
69 aberrant airway constriction response to allergen that is termed airway hypersensitivity or
70 hyperresponsiveness (AHR) ¹. Deregulation of airway smooth muscle cells (ASM), which play a
71 pivotal role in constriction and dilation of the airways, may be key to AHR ². ASM mass is greater
72 in patients with severe asthma compared to those with moderate asthma ³. Increased ASM mass
73 is also observed in children with severe asthma, despite having a relatively short duration of
74 asthma, suggesting that this change is directly linked with asthma severity ⁴. Moreover, ASM
75 isolated from asthmatics also exhibit enhanced contractile activity and enhanced proliferation ^{2,5}.
76 However, what drives these changes is still not fully appreciated.

77 Specifically, it has not been clear whether immune-mediated inflammatory signals into
78 ASM are directly responsible for lung dysfunction and if so which signals may be essential.
79 Several cytokines linked to asthma, notably IL-13, TNF, and IL-17, have been shown to promote
80 contractility or other responses in ASM in vitro, and can contribute to AHR in vivo in mouse models
81 ⁶⁻¹¹. Nevertheless, no data has yet shown that their direct actions on smooth muscle cells in vivo
82 are essential for ASM changes or for AHR in response to allergen. In particular, studies of the
83 receptor for IL-13, which has gained strong prominence in asthma pathogenesis from clinical trials
84 of the IL-4R α targeting antibody dupilumab ^{12,13}, failed to find a defect in AHR and smooth muscle
85 deregulation to allergen when IL-4R α was conditionally deleted in mice only in smooth muscle
86 cells ^{14,15}. Thus, the key molecules directly and dominantly controlling asthma-related changes in
87 ASM activity that are relevant for AHR are still not clear.

88 We previously linked the cytokine LIGHT (homologous to lymphotoxin, exhibits inducible
89 expression and competes with HSV glycoprotein D for binding to HVEM, a receptor expressed on
90 T lymphocytes), also known as TNF superfamily member 14 (TNFSF14), to the severity of lung
91 inflammation and to changes in ASM mass with studies of LIGHT-deficient mice ¹⁶. LIGHT can be

92 expressed by several immune cell types including activated T cells, dendritic cells, and neutrophils,
93 that are found in asthmatic lungs, and higher levels of soluble LIGHT or cell-associated LIGHT in
94 the sputum of asthmatic patients are associated with severe disease¹⁷⁻¹⁹. Structural cells of the
95 lung such as epithelial cells and fibroblasts express the receptors for LIGHT, namely HVEM
96 (TNFRSF14) and LT β R (LTBR/TNFRSF3), and LIGHT can promote inflammatory activity in these
97 cells²⁰⁻²⁴. However, whether LIGHT and its receptors act directly on airway smooth muscle cells
98 in vivo to promote exaggerated responsiveness and play a direct role in AHR has not been
99 demonstrated. In this study, we now show that LT β R is constitutively expressed on mouse and
100 human airway smooth muscle cells. With conditional deletion of LT β R in smooth muscle cells in
101 vivo, we demonstrate that LT β R activity in these cells is essential for smooth muscle remodeling,
102 lung dysfunction, and airway hyperresponsiveness driven by inhaled allergen. This is explained
103 by LT β R activating sustained signaling pathways involving NF κ B-inducing kinase (NIK) and
104 activation of non-canonical NF- κ B, pathways not triggered by the other ASM-associated cytokines
105 IL-13, TNF, and IL-17.

106

107 **METHODS**

108 **Mice**

109 C57BL/6J and smMHC (*Myh11*)/Cre/eGFP transgenic mice (B6.Cg-Tg(Myh11-cre,-
110 EGFP)2Mik/J)²⁵ were purchased from Jackson Laboratory. HVEM-floxed mice were generated
111 in-house as previously described^{23, 26}. LT β R-floxed mice were generated by Alexei Tumanov as
112 previously described²⁷. HVEM flox/flox or LT β R flox/flox mice crossed to smMHC^{Cre} transgenic
113 mice were bred in-house on the C57BL/6 background. Animal experiments were performed with
114 6–8-wk-old female mice. All animals used in this study were maintained in specific pathogen-free
115 conditions. All experiments were performed in compliance with the regulations of the La Jolla
116 Institute for Immunology Animal Care Committee in accordance with guidelines of the Association
117 for Assessment and Accreditation of Laboratory Animal Care.

118

119 **Mouse models of airway remodeling and acute airway inflammation**

120 For allergen airway remodeling experiments, mice were given intranasal administrations of
121 HDM, *Dermatophagoides pteronyssinus*, extract (Greer Laboratories, Lenoir, NC, USA): 200 μ g
122 on day 0 and 100 μ g on days 7 and 14, followed by 50 μ g of HDM given twice per week for 4
123 weeks. For LIGHT experiments, mice were injected intratracheally with 10 μ g of recombinant
124 LIGHT (R&D, Minneapolis, MN, USA) or PBS on day 1 and 2 and analyzed on day 3. For acute
125 airway inflammation, mice were sensitized by administration of 20 μ g HDM protein in 2mg alum
126 given intraperitoneally on day 0, and challenged with 10 μ g HDM protein intranasally on days 10-
127 13.

128

129 **Confocal microscopy of lung tissue**

130 Lungs were intubated, filled and embedded in the Cryomold with OCT compound, and frozen.
131 The fresh frozen lung tissues were post-fixed in 4% PFA and lung sections were cut (30 μ m) and
132 stained with rabbit polyclonal antibody to α SMA (alpha smooth muscle actin: Abcam, Cambridge,

133 UK), Phalloidin-AlexaFluor 568 (Thermo Fisher Scientific, Hampton, NJ, USA), and
134 Hoechst33342 (BD Bioscience, San Jose, CA, USA). All 3D high resolution tertiary bronchi image
135 stacks were acquired with an inverted Zeiss 780 or 880 Airyscan laser scanning confocal
136 microscope (LSCM) using a 40x (1.4na) objective and the 32-channel GaAsP-PMT area detector
137 (Zeiss Microscopy LLC, White Plains, NY, USA). Image stacks through 15-20 μm of lung tissue,
138 on average 35 slices, were acquired with Nyquist resolution parameters using a 0.421 μm step
139 size and optimal frame size of 2048x2048.

140 Lung tissue were further processed in imaris software using the isosurface module
141 (Bitplane) to outline and quantify the volume and area of α -smooth muscle actin or Phalloidin
142 around the mouse bronchioles. Phalloidin (F-actin) was more consistent in labeling the smooth
143 muscle, based on the density of the signal and circular localization pattern in addition to the
144 colocalization with αSMA . The actin labeling in all other non-muscle cells was omitted from
145 analysis by masking only the bronchioles using imaris software and then thresholding the F-actin
146 signal to omit very low to sparsely labeled F-actin in epithelial and other cells beyond the smooth
147 muscle layer. 10-15 tertiary bronchi per 4-5 mouse lungs per condition and mouse model were
148 analyzed.

149

150 **Airway hyperresponsiveness**

151 Airway resistance in response to different doses of Methacholine were measured using the
152 FlexiVent system (SCIREQ Inc, Montreal, Canada) as previously described ¹⁶. Peak airway
153 resistance was analyzed by Scireq flexiWare software V8.

154

155 **Flow cytometry**

156 Lungs were dissociated using gentleMACS Dissociator (Miltenyi Biotec, Bergisch
157 Gladbach, Germany) with Lung Dissociation Kit (Miltenyi Biotec). Single cells were stained with
158 monoclonal antibodies to mouse CD45 (clone:30-F11), CD11b (clone:M1/70), CD11c (clone:HL3),

159 SiglecF (clone: E50-2440) from BD Biosciences; EpCAM (clone:G8.8), CD31 (clone:390),
160 PDGFR α (clone:1A4/asm-1), Mcam (clone:ME-9F1) from BioLegend; vimentin (clone:280618)
161 from R&D; and α SMA (clone:1A4/asm-1) from Novus. Live/Dead cells were stained with Fixable
162 Aqua Dead Cell Staining Kit (Thermo Fisher). For intracellular staining, Foxp3 Transcription
163 Factor Staining Buffer Set (eBioscience, San Diego, CA, USA) were used for fixation and
164 permeabilization. Flow analysis was performed on a Fortessa (BD Biosciences) and data were
165 analyzed using FlowJo Software (version 10, FlowJo, LLC, Ashland, OR). Live⁺CD45⁺ lung
166 immune cells were gated for neutrophils, eosinophils, alveolar macrophages, CD4⁺ T cells and
167 CD8⁺ T cells following the gating strategy shown in the supplemental figure. Live⁺CD45⁻ lung
168 structural cells were gated as described in the figures into alternative populations by surface
169 staining for Epcam, CD31, PDGFR α , Mcam, and intracellular staining for vimentin and α SMA.

170

171 **Histology**

172 Whole lung lobes were fixed with 10% formalin and embedded in paraffin. Sections were stained
173 with hematoxylin and eosin or Periodic Acid-Schiff (PAS). Mucus production was assessed by
174 measuring the percentage of PAS-positive cells airway epithelial cells in the bronchioles. More
175 than 5 bronchi per section were randomly selected and used for quantification.

176

177 **BAL cytokines**

178 Cytokines in BAL fluid were assayed by sandwich ELISA with paired antibody sets, according to
179 the manufacturers' instructions. Mouse IL-4, IL-5 and IL-13 kits were from R&D.

180

181 **ASM culture and analysis**

182 Healthy donor human ASM or asthmatic diseased donor ASM were purchased from ScienCell
183 (cat:3400; Carlsbad, CA, USA) or Lonza (cat: 00194850; Walkersville, MD, USA). Cells from
184 several donors were used for reproducibility. Other asthmatic donor ASM were isolated from

185 postmortem lungs provided by Richard Kurten from the Arkansas Regional Organ Recovery
186 Agency as previously described²⁸. HI129: Asthma, 7 years old, Male, Caucasian, Non-smoker,
187 COD CVA/Stroke; HI227: Asthma, 21 years old, Male, Caucasian, Non-smoker, COD Head
188 trauma. For flow analyses, cells were stained with monoclonal antibodies to human LT β R
189 (clone:31G4D8), or HVEM (clone:122) from BioLegend. Cells were maintained in Smooth Muscle
190 Cell Media (ScienCell) with supplied supplements and FBS added. Cells were used between
191 passages 2–4 and cultured in smooth muscle basal media for 16 hours or 7 days before
192 stimulation with recombinant LIGHT (100 ng/ml). In some experiments, inhibitors of NIK/non-
193 canonical NF- κ B (NIK-SMI, 25nM, MedChemExpress, Monmouth, NJ, USA), canonical NF- κ B
194 (BAY11-7082, 1nM, MedChemExpress), or Rac1 (NSC 23766, 10nM, Tocris, Birstol, UK) were
195 added for 1 hour before stimulation with rLIGHT. For siRNA knockdown, ON-TARGETplus siRNA
196 to human LT β R and NIK, and an NTC control, were purchased from Dharmacon (Pittsburg, PA,
197 USA). siRNA Oligo Duplex siRNA to human HVEM was purchased from Origene (Rockville, MD,
198 USA). 50 nM of siRNA was transfected into ASM using HiPerFect transfection reagent (Qiagen,
199 Venlo, Netherlands) as described previously²¹ and according to the manufacturer's instructions.

200

201 **ASM gel contraction assay**

202 3D Gel contraction assays were performed using collagen contraction assay kits purchased from
203 Cell Biolabs (San Diego, CA, USA) according to the manufacturer's instructions. In brief,
204 suspensions of ASM were mixed with collagen solution at a density of $0.5-1 \times 10^6$ cells/well. After
205 confirming the polymerization of collagen gels, smooth muscle basal media was added and
206 incubated for 16 hours. Collagen gels were then stimulated with rLIGHT (100 ng/ml), rLT $\alpha\beta$ (100
207 ng/ml) or PBS and analyzed for gel contraction at different timepoints (24, 48, 72 hours). Images
208 were obtained with ImageLab (Bio-Rad Laboratories, Hercules, CA) and the area of collagen gel
209 matrix measured using ImageJ software.

210

211 ASM intracellular protein analysis

212 For analyzing actin polymerization and focal adhesions, ASM were incubated in smooth muscle
213 basal media without serum for 16 hours and seeded as monolayers at 70-80% confluency on
214 coverslips coated with Collagen Type I solution (Sigma-Aldrich, St. Louis, MO, USA). Cells were
215 stimulated with 100 ng/ml of rLIGHT or PBS with or without NIK-SMI or Rac inhibitors. After 6-12
216 hours, cells were washed and fixed with 4% Formalin and permeabilized with 0.1% TritonX-100
217 (Thermo Fisher Scientific). Cells were stained with Phalloidin-Alexa Fluor 568 (Thermo Fisher
218 Scientific), anti-Vinculin antibody (Abcam) and Hoechst 33342 (BD Bioscience) and analyzed by
219 confocal microscopy. Single ASM images were processed in imaris software using the isosurface
220 module (Bitplane) to outline and quantify the volume of intracellular vinculin clusters and F-actin
221 expression (Phalloidin). All 3D high resolution single ASM cell images were acquired with an
222 inverted 880 Airyscan laser scanning confocal microscope (LSCM) using a 63x (1.4na) objective
223 and the 32-channel GaAsP-PMT area detector (Zeiss Microscopy LLC). Image stacks through 3-
224 5 μm of spreading ASM, on average 10-15 slices, were acquired with Nyquist resolution
225 parameters using a 0.3 μm step size and optimal frame size of 4164x4164. 300-400 individual
226 ASM, in two replicate experiments for the various conditions, were analyzed.

227

228 ASM migration/wound assay

229 ASM were seeded in monolayers on coverslips coated with Collagen Type I solution (Sigma-
230 Aldrich) and cultured in smooth muscle media until reaching 90% confluency. Cells were
231 incubated in smooth muscle basal media for 16 hours before making a scratch wound in a straight
232 line followed by washing out of any debris. Smooth muscle basal media containing 100 ng/ml of
233 rLIGHT or PBS was then added and incubated for 12 hours. Cells were washed and fixed with
234 4% Formalin and permeabilized with 0.1% TritonX-100 (Thermo Fisher Scientific). Cells were
235 stained with Phalloidin-Alexa Fluor 568 (Thermo Fisher Scientific) and Hoechst 33342 (BD

236 Bioscience) and analyzed by confocal microscopy. All 3D multi-stitched image panels were
237 acquired on an inverted Zeiss LSM 780 LCSM using a 20x 0.8 NA objective, a z-step size of 0.85
238 microns and by using the automated tiling function of the Zen software with a 10% overlap
239 between tiles. Images were stitched and 3D stacks were maximum intensity projected using the
240 Zen software then imported into Image Pro Premier 10 (IPP10) Media Cybernetics) for further
241 processing. Briefly, by using the phalloidin-AF555 signal to define the cells along the wound edge
242 and the thresholding tool in IPP10 to define areas devoid of cells (set at a dynamic range of 0-50
243 for 8 bit images), the auto count tool automatically outlined and quantified the area all along the
244 wound front, allowing quantification of the wound area and the extent of ASM migration into the
245 wound.

246

247 **ASM proliferation**

248 ASM were cultured in the presence of 100 ng/ml rLIGHT or PBS. After 48 hours, cells were
249 harvested and the proliferating cells were detected by BrdU incorporation using a FITC BrdU Flow
250 Kit (BD Bioscience) according to the manufacturer's protocol.

251

252 **Western Blotting**

253 Cells were lysed in RIPA Buffer containing protease inhibitor (Roche, Mannheim, Germany)
254 Whole cell lysates were run in WedgeWell 8-16% Tris-Glycin gradient gels (Novex) and
255 transferred to Nitrocellulose membrane (Bio-Rad). Membranes were incubated with 5% BSA
256 (Sigma-Aldrich) or non-fat dry milk (R&D) in TBS-T for blocking, then incubated with primary
257 antibodies to p-NFκB p65 (cat:3033, 1:1000), NFκB p65 (cat:8242, 1:1000), NFκB p100/52
258 (cat:3017, 1:1000), PAK1 (cat:2602,1:1000), p-MYPT(Thr696) (cat:5163, 1:1000), p-MLC2
259 (cat:3672, 1:1000), MLC2 (cat:8505, 1:500) from Cell Signaling Technology; to p-PAK1
260 (cat:135755, 1:200) and MYPT (cat:514261, 1:100) from Santa Cruz; followed by HRP-
261 conjugated secondary antibodies to mouse IgG (cat:516102, Santa Cruz) or rabbit IgG (cat:2357,

262 Santa Cruz). Chemiluminescence was enhanced with Amersham ECL Prime Western Blotting
263 Detection Reagent (GE Health Care, Madison, WI, USA) and visualized after exposure to Gel
264 Doc (Bio-Rad). Stripping and reblotting were performed with Restore Western Blot Stripping
265 Buffer (Thermo Fisher Scientific). Immunoblotting for GAPDH (Santa Cruz, Dallas, TX, USA) was
266 used as loading control. For Rac1 detection, whole cell lysates were used for immunoprecipitation
267 using Active Rac1 detection kit (Cell Signaling Technology, Danvers, MA, USA) according to the
268 manufacturer's instruction.

269

270 **RT-PCR**

271 Total RNA from ASM was isolated using RNeasy kit (Qiagen). cDNA was prepared using a
272 SuperScript IV reverse transcriptase kit (Thermo Fisher Scientific). Real-time PCR was performed
273 with LightCycler (Roche, Indianapolis, Ind) using PowerUp SYBR Green master mixes (Applied
274 Biosystems, Foster City, CA). Data were normalized with housekeeping gene GAPDH and
275 presented as relative expression or relative quantification to control samples which were derived
276 from the difference in cycle threshold (Ct) between the gene of interest and the housekeeping
277 genes using the equation $RQ = 2^{-\Delta\Delta Ct}$. Designed primers for human MAP3K14 were purchased
278 from Bio-Rad (Hercules, CA, USA). The oligonucleotide primer sequences were: GAPDH, sense
279 AGCCAAAAGGGTCATCATCTCT, anti-sense AGGGGCCATCCACAGTCTT; HVEM, sense
280 AGCAGCTCCCACTGGGTATG, anti-sense GATTAGGCCAACTGTGGAGCA; LT β R, sense
281 CCGACACAACCTGCAAAAAT, anti-sense GAGCAGAAAGAAGGCCAGTG.

282

283 **Analysis of published RNA-seq data**

284 Bulk RNA-seq of healthy and asthma ASM were analyzed for transcripts of cytokine receptors.
285 Fong et al ²⁹⁻³¹ used ASM from 11 asthmatic and 12 non-asthmatic donors over two GEO
286 submissions: GSE119578 (GSE119578_GeneCount_rpk_m_by_gene_RDB.txt.gz) and
287 GSE119579 (GSE119579_GeneCount_rpk_m_by_gene_SW.txt.gz). Himes et al ²⁹⁻³¹ used ASM

288 from 6 donors with fatal asthma and 12 control donors. Only baseline (no treatment)
289 measurements from GSE58434 were analyzed (GSE58434_All_Sample_FPKM_Matrix.txt.gz).
290 Kan et al (Kan et al., 2019) used ASM from 9 fatal asthma and 8 non-asthma donors. Only vehicle
291 control samples from GSE94335 were analyzed (GSE94335_PostQC_all_sample_TPM.txt.gz).

292

293 **Statistical analysis**

294 All results are presented as mean \pm SEM. Statistical significance was analyzed by Mann-Whitney
295 test for comparison of means between 2 independent groups or by 1-way ANOVA followed by
296 Tukey's post hoc multiple comparison test for differences of means between multiple groups using
297 Prism 8 software (GraphPad Prism, San Diego, CA). P value <0.05 was considered statistically
298 significant. *P < 0.05 , **P < 0.01 , ***P < 0.001 , ****P < 0.0001 .

299

300 RESULTS

301 **LT β R and HVEM are expressed on ASM from healthy and asthmatic individuals**

302 We first studied expression of the receptors for LIGHT, LT β R and HVEM, in published
303 RNA-seq data from airway smooth muscle cells (ASM) isolated from healthy and asthmatic
304 individuals²⁹⁻³¹. Three separate data sets revealed strong expression of transcripts for LT β R and
305 lower levels of transcripts for HVEM (**Fig. 1A**). Interestingly, compared to the receptors for the
306 three primary asthma-related cytokines linked to activities in airway smooth muscle cells, namely
307 TNFR1, IL4R, and IL17RA and IL17RC, only TNFR1 transcripts were as, or more, abundant
308 compared to LT β R transcripts. No differences in transcript levels were observed for any of the
309 receptors between healthy and asthmatic ASM (**Fig. 1A**). Flow cytometric analyses of two
310 preparations of ASM from healthy individuals obtained from commercial sources confirmed that
311 LT β R was more strongly expressed on the cell surface than HVEM. Analysis of ASM from
312 asthmatic subjects, from a commercial source and from post-mortem lungs of asthmatics isolated
313 in-house, furthermore showed equivalent expression of both molecules compared to healthy
314 donor ASM, with LT β R being most highly expressed (**Fig. 1B**).

315

316 **ASM-specific LT β R-deficient mice display reduced ASM mass and AHR in allergen- 317 induced experimental asthma**

318 To then assess the importance of LT β R or HVEM on ASM in vivo, we used smooth muscle
319 Myosin Heavy Chain (smMHC)^{Cre} (*Myh11*)-eGFP transgenic mice²⁵. Similar to human cells, each
320 receptor was expressed constitutively on ASM in the mouse lungs (**Fig. 2A**). We next generated
321 smooth muscle cell-specific receptor knockout mice by crossing smMHC^{Cre} mice to HVEM^{fl/fl} or
322 LT β R^{fl/fl} mice, and confirmed deletion of each receptor in ASM after gating on lung GFP-smMHC
323 positive cells (**Fig. 2A**). Previous studies using scRNAseq have revealed several markers to
324 identify structural cell subsets in the lung^{32,33}, however there is still a lack of an established gating

325 strategy to identify ASM by conventional flow cytometric methods without a marker tag. We found
326 that among the CD45⁻ EpCAM⁻ PDGFR α ⁻ and Vimentin^{low} population, that excludes epithelial and
327 endothelial cells and fibroblasts, there are two distinct α SMA (alpha smooth muscle actin) positive
328 populations subdivided based on MCAM (CD146) expression (**Fig. E1A**). MCAM is known to be
329 highly expressed on pericytes and lower in smMHC⁺ mature smooth muscle cells³⁴. By analyzing
330 the smMHC^{Cre} conditional knockout mice, we found that both HVEM and LT β R were deficient in
331 the α SMA⁺ MCAM⁻ population, but not the α SMA⁺ MCAM⁺ population or in fibroblasts or epithelial
332 cells. This further showed the specificity of the conditional deletion of the two receptors and
333 revealed that ASM can be distinguished effectively as CD45⁻ EpCAM⁻ PDGFR α ⁻ Vimentin^{low}
334 α SMA⁺ MCAM⁻ cells in the lungs (**Fig. E1B**).

335 The conditional knockout mice and control animals (smMHC^{Cre}) were then exposed to
336 chronic repetitive intranasal challenges with house dust mite allergen extract over 6 weeks in a
337 model of asthma that results in airway remodeling. Similar to what we previously reported¹⁶, the
338 allergen drove an eosinophilic inflammatory response in the lungs of control animals,
339 accompanied by a strong increase in bronchial ASM mass, as visualized and quantified by high-
340 resolution 3-dimensional confocal microscopy of the immunofluorescent staining of α SMA and
341 phalloidin (Filamentous actin). These changes were associated with profound airway
342 hyperresponsiveness, reflected by increased lung resistance to methacholine when administered
343 intranasally (**Fig. 2B-G**). Strikingly, we found that no significant increase in bronchial ASM mass
344 was observed in ASM-specific LT β R-deficient mice compared to the approximate doubling in
345 mass seen in control animals when quantified by histological analysis (**Fig. 2B-C**). In contrast, a
346 normal smooth muscle response to allergen was found in mice specifically lacking HVEM in ASM.
347 Importantly, AHR was strongly reduced in LT β R conditional knockout mice challenged with
348 allergen whereas AHR was induced in HVEM conditional knockout mice comparable to control
349 wild-type mice (**Fig. 2D**).

350 Flow cytometry analysis of dissociated lung tissue cells furthermore revealed another
351 specific requirement for $LT\beta R$ in controlling ASM. While the total number of smooth muscle cells
352 was enhanced in the lungs of allergen-exposed smMHC^{Cre} and ASM-specific HVEM-deficient
353 mice, no increase was found in $LT\beta R$ -deficient mice (**Fig. 2E**). Moreover, demonstrating that this
354 was not a bystander effect of a poor inflammatory response, the number of inflammatory cells,
355 including eosinophils, that accumulated in the lung tissue, and the overall infiltrates around the
356 bronchioles, as well as Th2 cytokine production in BAL fluid, were not different between the control
357 and $LT\beta R$ conditional knockout mice challenged with allergen (**Fig. 2F-G, Fig. E2A-B**). Mucus
358 production determined by PAS staining of bronchial epithelium was also not different between the
359 control and $LT\beta R$ conditional knockout mice challenged with allergen (**Fig. E2C**).

360 Thus, $LT\beta R$ controlled hyperplasia and hypertrophy of ASM in the context of chronic
361 repetitive airway allergen exposure, and this strongly contributed to the development of AHR and
362 lung dysfunction. Importantly, the latter was dissociated from generalized inflammation
363 demonstrating the requirement for direct signals to smooth muscle cells.

364 We also assessed if $LT\beta R$ played a role in AHR in an acute asthma model without chronic
365 repetitive allergen exposure, where airway remodeling does not occur to any extent. In this case,
366 only a weak AHR response resulted in control mice challenged with HDM. However, this was
367 reduced in $LT\beta R$ conditional knockout mice to the level seen in naïve unchallenged mice (**Fig.**
368 **E2D**). Together, this suggests that the primary effect of $LT\beta R$ on AHR is explained by its action
369 on driving ASM remodeling, but that $LT\beta R$ might also control ASM contractility in the absence of
370 significant remodeling.

371

372 **LIGHT- $LT\beta R$ signals increase ASM mass and AHR in vivo**

373 The above findings in allergen-induced airway remodeling correlated with the reduction in
374 airway smooth muscle mass we found in LIGHT-deficient mice ¹⁶. To directly relate the results to

375 the activity of LIGHT as a cytokine, we then injected rLIGHT at a high dose intratracheally into
376 unimmunized control and conditional knockout mice over 3 days. The smooth muscle layer was
377 again quantified by high-resolution 3-dimensional confocal microscopy (**Fig. E3A**). Replicating
378 our observations from two previous studies^{16, 24}, rLIGHT administration to the lungs induced a
379 significant increase in smooth muscle mass surrounding the bronchi in control mice (**Fig. 3A-B**).
380 Importantly, this increased ASM mass was not observed in mice with conditional deletion of LT β R
381 in ASM, whereas ASM specific-deletion of HVEM did not diminish the LIGHT-driven response
382 compared to that in smMHC^{Cre} control mice (**Fig. 3A-B**).

383 To extend this data, we quantified the number of total lung smooth muscle cells by flow
384 cytometry as before. In this case, intratracheal rLIGHT administration did not alter the number of
385 ASM, as well as having no effect on promoting increased numbers of total cells and eosinophils
386 in the lung tissue (**Fig. E3B**). Thus, the primary action of recombinant LIGHT in this setting in vivo
387 was to promote ASM hypertrophy, suggesting that the LT β R-driven hyperplasia seen with
388 repetitive allergen exposure (Fig. 2E) may have been dependent on other inflammatory factors
389 elicited by the allergen acting together with LIGHT. However, regardless of the latter, rLIGHT
390 injection still significantly induced AHR, albeit less than that seen with repetitive allergen (**Fig. 3C**,
391 compare to Fig. 2D). Most importantly, ASM-specific LT β R-deficient animals displayed strongly
392 reduced AHR, unlike HVEM-deficient animals that showed similar AHR compared to the control
393 mice treated with rLIGHT (**Fig. 3C**). These results collectively demonstrate that LIGHT can signal
394 through LT β R on ASM in the lungs and directly drive smooth muscle hypertrophy and lung
395 dysfunction (**Fig. 3**), and in the context of a response to allergen the LT β R signal is also critical
396 and dominant for smooth muscle hyperplasia leading to even greater lung dysfunction associated
397 with airway remodeling (**Fig. 2**).

398

399 **LIGHT-LT β R interactions promotes contractile activity, hypertrophy, and hyperplasia in**
400 **human ASM**

401 To further investigate the direct actions of LIGHT-LT β R signals on airway smooth muscle
402 cells, we analyzed normal human primary bronchial smooth muscle cells. Indicating that LT β R
403 was active, it was downregulated after culture with LIGHT, a phenomenon previously associated
404 with initiation of signaling through this receptor (**Fig. 4A**). The human ASM were then cultured in
405 3D collagen gels to make a net structure (**Fig. 4B**) and stimulated with LIGHT to assess contractile
406 activity. Significantly, LIGHT induced strong activity in this assay shown by shrinking of the
407 collagen gel, largely seen from 24-48 hours (**Fig. 4C**). In line with the notion that this was due to
408 LT β R signaling, knockdown of this receptor with siRNA, but not knockdown of HVEM, prevented
409 LIGHT-induced contractile activity (**Fig. E4A-B**). The membrane version of lymphotoxin, LT $\alpha\beta$, is
410 also a ligand of LT β R. Recombinant LT $\alpha\beta$ induced identical gel contraction compared to LIGHT
411 (**Fig. E4C**), further supporting the dominant role of LT β R in driving smooth muscle cell activity.

412 We next assessed whether LIGHT-LT β R interactions can promote proliferation of ASM.
413 Functional changes in cultured ASM have been studied previously with both contractile and
414 synthetic/proliferative phenotypes observed dependent on culture conditions.
415 Synthetic/proliferative cells can mature into contractile cells by prolonged serum deprivation². We
416 thus compared early passage human ASM with a proliferative phenotype to those with a
417 contractile phenotype cultured without serum for 7 days. By assessing BrdU incorporation,
418 proliferative ASM exhibited a high background rate of BrdU uptake (**Fig. 4D**), and this was
419 enhanced significantly by LIGHT stimulation. Contractile ASM weakly incorporated BrdU, which
420 was less strongly, albeit significantly, affected by LIGHT (**Fig. 4D**). Lastly, human ASM
421 hypertrophy was assessed in vitro, and LIGHT significantly increased the volume of individual
422 cells (**Fig. 4E**), again corresponding to the in vivo phenotype observed in the mouse (Figs. 2 and
423 3).

424

425 LIGHT increases actin polymerization in ASM

426 Contractile force in smooth muscle cells is generated by ATP-dependent interaction
427 between F-actin and myosin, regulated in part by phosphorylation of myosin light chain by myosin
428 light chain kinase (MLCK). In asthmatic patients, in addition to increased numbers of the
429 contractile actin/myosin-expressing ASM subset, upregulation of MLCK and other proteins
430 associated with MLCK activity has been reported⁵. Furthermore, cell hypertrophy is also directly
431 related to several factors associated with contractility, including actin polymerization, as is
432 migration of ASM, another process thought relevant to ASM mass changes in asthma³⁵.

433 We therefore first assessed by RNA-seq whether LIGHT might promote responsiveness
434 in ASM by regulating the expression of contractile molecules and signaling molecules associated
435 with contraction. We did not detect any upregulation of transcripts for such molecules including
436 alpha smooth muscle actin, contractile myosin heavy chain 11 isoform, and RhoA (**Fig. 5A**). In
437 contrast, by GSEA, we found significant enrichment by LIGHT of transcriptional machinery
438 associated with the cell membrane and actin rearrangement (**Fig. 5B**). This led us to focus on the
439 quantitative analysis of intracellular F-actin and vinculin expression which reflect cytoskeletal
440 macromolecular changes associated with mechanical force, migration, and hypertrophy. By
441 confocal imaging analysis, human ASM stimulated with LIGHT were found to significantly
442 increase the volume of vinculin rich focal adhesions and polymerized F-actin rich stress fibers
443 compared to unstimulated cells within 6-12 hr (**Fig. 5C**). Further in line with this, migration of ASM
444 was enhanced by LIGHT stimulation in migration/wound assays of monolayers assayed at 12hr,
445 correlating with increased expression of actin filaments (**Fig. 5D**). Thus, overall, these results
446 suggested that actin polymerization might have been central to many or all of the activities of
447 LT β R on driving ASM dysregulation.

448

449 LIGHT-induced non-canonical NF- κ B signaling induces actin polymerization in ASM

450 As $LT\beta R$ signals are known to induce both early onset canonical NF- κB activation, as well
451 as late onset non-canonical NF- κB activation, in other cell types, we asked if one or both of these
452 pathways were activated by LIGHT in human ASM. Indeed, LIGHT stimulation induced a small
453 increase in phosphorylation of p65 (canonical NF- κB) after 15 mins. However, most interestingly,
454 LIGHT resulted in processing of p100 to p52 (the signature of non-canonical NF- κB pathway
455 activation) starting ~4 hrs after stimulation and extending to 24 hrs (**Fig. 6A**). We then assessed
456 whether LIGHT-induced non-canonical NF- κB signaling was required for actin rearrangement and
457 contractile activity using NIK-SMI, an inhibitor of NF- κB -inducing kinase (NIK), the kinase that is
458 central to p100 processing into p52³⁶. Treatment with NIK-SMI significantly reduced LIGHT-
459 induced actin polymerization although it did not block the increase in focal adhesions (**Fig. 6B**).
460 Moreover, NIK-SMI also effectively prevented LIGHT-induced contractile activity visualized in 3D
461 collagen gels, whereas in contrast, BAY11-7082, a canonical NF- κB inhibitor, had no effect on
462 LIGHT-induced gel contraction (**Fig. 6C**). Knockdown of NIK (Map3k14) with siRNA further
463 supported the inhibitor studies and prevented LIGHT-driven gel contraction (**Fig. E4A-B**). Notably,
464 non-canonical signaling, initiated from 4hr and sustained at least up to 24hr (Fig. 6A), preceded
465 the initiation of contraction at 24hr (Fig. 4C and S4), and preceded or coincided with changes in
466 actin polymerization and migration related to actin polymerization (Fig. 5C and D), reinforcing the
467 conclusion regarding the relevance of this pathway from the NIK inhibition assays. Thus, LIGHT-
468 $LT\beta R$ dependent non-canonical NF- κB signaling is central to dysregulation of ASM. Moreover,
469 distinguishing LIGHT from other cytokines reported to be capable of acting on ASM, namely IL-
470 13, TNF, and IL-17, none of these cytokines induced non-canonical NF κB activation in ASM (p52
471 processing), even though canonical NF- κB (pp65) was induced, particularly by TNF, as previously
472 reported (**Fig. E5**).

473

474 **LIGHT induces actin polymerization and sustained phosphorylation of MLC via non-**
475 **canonical NF- κ B activation of Rac1/PAK1**

476 To further understand the role of non-canonical NF- κ B signaling, we examined other
477 changes associated with activity in ASM. Phosphorylation of myosin light chain (MLC) is regulated
478 directly by MLC kinase and MLC phosphatase, and a Rho-dependent pathway inhibits MLC
479 phosphatase whereas calcium dependent calmodulin signaling activates MLC kinase^{5, 37}. LIGHT
480 promoted phosphorylation of MLC in human ASM within 5 minutes but importantly it sustained
481 MLC phosphorylation over 24 hrs (**Fig. 7A**). We also detected late and sustained phosphorylation
482 of the serine threonine kinase PAK1 (p21-activated kinase 1) over 24 hrs, that is a target of the
483 GTP binding protein Rac1, and has been implicated in cytoskeleton/actin reorganization as well
484 as being upstream of MLC kinase (**Fig. 7B**). Consistent with this, the active (GTP) form of Rac1,
485 bound to PAK1, was detected between 1-4 hours after LIGHT stimulation (**Fig. 7C**). We also
486 assessed phosphorylation of MYPT (a subunit of MLC phosphatase) downstream of the Rho-
487 dependent pathway³⁸, but in this case LIGHT induced only early transient and weak
488 phosphorylation of MYPT at 15 mins (**Fig. 7B**).

489 Since PAK1 has been reported to interact with NIK³⁹, we hypothesized that the late
490 phosphorylation of MLC and activation of Rac1/PAK1 was also related to non-canonical NF- κ B
491 signaling. Indeed, LIGHT-induced phosphorylation of PAK1 (**Fig. 7D**) and sustained
492 phosphorylation of MLC (**Fig. 7E**) was reduced by NIK inhibition in a dose-dependent manner.
493 Correspondingly, inhibiting NIK also prevented LIGHT from promoting the binding of active Rac1
494 to PAK1 (**Fig. 7F**). Lastly, to further consolidate the significance of this signaling pathway to ASM
495 dysfunction, we found that a Rac1 inhibitor blocked LIGHT-induced contraction in 3D gels (**Fig.**
496 **7G**). Correspondingly treatment with the Rac1 inhibitor reduced actin polymerization, and in this
497 case also blocked the increase in focal adhesions driven by LIGHT (**Fig. 7H**).

498 Together with our in vivo data, these results indicate that LT β R-induced non-canonical
499 NF- κ B signaling is a primary and dominant driver of airway smooth muscle cell
500 hyperresponsiveness.

Journal Pre-proof

501 **DISCUSSION**

502 Airway smooth muscle cells have long been considered to be central for lung dysfunction
503 in asthma due to their ability to narrow the airways. However, whether there are dominant
504 receptors on ASM that explain ASM remodeling that is seen in severe asthma and explain airway
505 hyperresponsiveness has not been clear. Our present study now reveals the novel finding that
506 $LT\beta R$ is essential for allergen-driven ASM remodeling and the resultant increased airway
507 hyperresponsiveness that is associated with remodeling. Importantly, to our knowledge, out of
508 the primary cytokine receptors that have been associated with asthma and ASM activity, namely
509 those for IL-13, TNF, and IL-17, this is the first study to show that deletion of a single cytokine
510 receptor only on smooth muscle cells can strongly impact ASM deregulation and AHR in response
511 to allergen in vivo. This correlates with the unique ability of $LT\beta R$ to drive non-canonical NF- κB
512 signaling, an activity not shared by these other cytokine receptors. The results have major
513 implications for our understanding of the control of airway remodeling and hyperresponsiveness
514 in asthma.

515 We favor the notion that LIGHT, rather than $LT\alpha\beta$ the other ligand for $LT\beta R$, is the primary
516 factor relevant for smooth muscle remodeling. Higher expression of LIGHT has been reported in
517 the sputum of severe asthmatic patients¹⁷⁻¹⁹, and in previous studies of LIGHT-deficient mice we
518 showed that this cytokine participated in remodeling of the ASM mass that was induced by
519 repetitive exposure to allergen¹⁶. LIGHT-deficient mice were protected from ASM remodeling at
520 a similar level as WT mice treated with $LT\beta R.Ig$ that blocks both LIGHT and $LT\alpha\beta$ ¹⁶, further
521 implying that at least in our mouse model systems LIGHT is the primary ligand. However, it is
522 possible that $LT\alpha\beta$ could be important in human asthmatics as it is capable of inducing the same
523 signals as LIGHT through the $LT\beta R$, and thus we cannot definitively rule out a contribution of
524 $LT\alpha\beta$.

525 Increased ASM mass has previously been related to the severity and baseline lung
526 function in patients with asthma ³ with ASM hyperplasia and an increased number of bronchial
527 ASM being well established as features of asthmatic airways ³⁵. Although ASM hypertrophy in
528 asthma is less discussed ³⁵, asthmatic bronchial biopsies have been found to contain smooth
529 muscle cells of larger diameter compared to control subjects, and severe asthmatics presented
530 with the highest smooth muscle cell size ⁴⁰. Our data here show that LIGHT-LT β R promoted both
531 ASM hyperplasia and hypertrophy in vivo and in vitro. LIGHT drove only moderate proliferation in
532 cell culture but LT β R signals to ASM were essential for the increased number of lung smooth
533 muscle cells seen in vivo in response to allergen. In addition, LIGHT directly promoted an increase
534 in ASM size in vitro accompanied by increased actin polymerization, and in vivo, recombinant
535 LIGHT administration without other inflammatory signals increased peribronchial ASM mass
536 without affecting the total number of lung ASM. Thus, these observations strongly imply that LT β R
537 signals could be central to both smooth muscle cell hyperplasia and hypertrophy seen in asthma.

538 The finding that LT β R activates the non-canonical NF- κ B pathway in ASM and drives
539 sustained changes in actin polymerization and rearrangement distinguishes it from the other
540 primary cytokine receptors that have been described to also induce ASM responses in vitro,
541 namely those for IL-13, TNF, and IL-17 ⁴¹. Non-canonical NF- κ B signaling is a late-onset and
542 more continual inflammatory signal reliant on recruitment of the NF- κ B-inducing kinase, NIK. TNF
543 via canonical NF- κ B was found to induce activation of RhoA in ASM leading to inhibition of MLC
544 phosphatase ^{9, 42}. IL-13 was shown to upregulate the expression of RhoA or enhance Ca²⁺
545 signaling dependent on STAT6, MAPK, and PI3K activity ^{7, 43-46}. Moreover, IL-17 was also found
546 to drive migration, contraction, or other activities in ASM, dependent on several MAPK pathways,
547 canonical NF- κ B, and PKC ⁴⁷⁻⁴⁹. Thus, while these cytokine receptors might then promote other
548 signaling pathways compared to LT β R, or in the case of the receptors for TNF and IL-17 impact
549 canonical NF- κ B activation similar to LT β R, they have not been described to activate NIK, and we

550 show they do not drive p100 processing to p52 in ASM. Therefore, they are more likely to trigger
551 early and transient activities compared to LT β R.

552 Collectively, this suggests that LT β R signaling can differ from the actions of these other
553 cytokine receptors in engendering sustained increases in ASM mass and a contractile phenotype.
554 This could explain the dominant effect of deleting the LT β R in smooth muscle cells that we
555 observed in vivo. Our data however do not rule out important contributions for these other cytokine
556 receptors on ASM in asthma, simply that LT β R signaling in the context of allergen is essential. In
557 fact, recent results with mice with conditional deletion of IL-4R α in both epithelial cells and smooth
558 muscle cells supports a role for IL-13 and IL-4R in control of ASM albeit dependent on epithelial
559 cell activity⁵⁰. We suggest that LIGHT might act on ASM in concert with these other cytokines,
560 dependent on their production and availability within the lung, given that IL-13, IL-17 and TNF are
561 also products of T cells and other inflammatory cells that can make LIGHT. We previously
562 reported that LIGHT stimulated IL-13 production from eosinophils in experimental asthma models
563¹⁶, and that injection of LIGHT into the naive lungs also upregulated IL-13, potentially from ILC,
564 coincident with a partial requirement for IL-4R α in promoting ASM mass²⁴, both observations that
565 are in line with LIGHT working together with IL-13 to amplify smooth muscle responsiveness.
566 Whether LIGHT co-operates with TNF or IL-17 to regulate ASM activities has not been shown yet,
567 but it will be interesting in future studies to fully understand the extent of cross-talk and synergy
568 between these cytokines on ASM.

569 In summary, our study reveals direct evidence that LT β R, most likely activated by LIGHT,
570 can drive ASM hypertrophy, hyperplasia, and contractile activity, and is essential for airway
571 hyperreactivity that results after chronic exposure to airway allergen. The data suggest that
572 signaling through LT β R is critically required for smooth muscle changes and AHR regardless of
573 the potential for other cytokines to be active, as shown by the almost complete lack of ASM
574 hypertrophy, hyperplasia, and airway hyperresponsiveness in allergen-challenged mice where

575 LT β R was specifically deleted in smooth muscle cells. Existing asthma treatments largely target
576 inflammatory cells such as eosinophils or mast cells, and airway constriction is only transiently
577 controlled by beta agonist inhalers. Blocking LIGHT-LT β R interactions, and possibly LT $\alpha\beta$ -LT β R
578 interactions, or disrupting non-canonical NF- κ B signaling in smooth muscle cells, could represent
579 important therapeutic approaches for persistent and chronic airway hyperresponsiveness in
580 severe asthmatic patients or patients with similar lung dysfunction.

581

Journal Pre-proof

582 Author Contributions

583 H.M. designed and conducted experiments, and wrote the paper. W.B.K designed and conducted
584 experiments. M.M, M.C.M, R.H, R.D.S.A, R.K.G and G.S.S assisted with assays or experiments.
585 K.F and A.S performed bioinformatics analysis. P.D and F.A analyzed published RNA-seq data.
586 K.D. assisted histology studies. M.M and D.H.B provided human ASM and assisted with assay
587 design. A.V.T provided mice. M.C directed the study, designed experiments, and wrote the paper.

588

589 Acknowledgements

590 This study was supported by NIH grant AI070535 to MC.

591 HM was supported by an JSPS Overseas Research Fellowship, and JSPS KAKENHI Grant
592 Number JP22K20924.

593 We would like to thank Jaqueline Miller for technical support, Richard Kurten for providing post-
594 mortem lung slices for ASM isolation, Alexa Pham for assistance with ASM isolation, and Mitch
595 Kronenberg for originally providing HVEM-floxed mice.

596

597 **References**

- 598 1. Busse WW, Lemanske RF, Jr. Asthma. *N Engl J Med* 2001; 344:350-62.
- 599 2. Zuyderduyn S, Sukkar MB, Fust A, Dhaliwal S, Burgess JK. Treating asthma means
600 treating airway smooth muscle cells. *Eur Respir J* 2008; 32:265-74.
- 601 3. Pepe C, Foley S, Shannon J, Lemiere C, Olivenstein R, Ernst P, et al. Differences in
602 airway remodeling between subjects with severe and moderate asthma. *J Allergy Clin*
603 *Immunol* 2005; 116:544-9.
- 604 4. Kaminska M, Foley S, Maghni K, Storness-Bliss C, Coxson H, Ghezzi H, et al. Airway
605 remodeling in subjects with severe asthma with or without chronic persistent airflow
606 obstruction. *J Allergy Clin Immunol* 2009; 124:45-51.e1-4.
- 607 5. Mahn K, Ojo OO, Chadwick G, Aaronson PI, Ward JP, Lee TH. Ca(2+) homeostasis and
608 structural and functional remodelling of airway smooth muscle in asthma. *Thorax* 2010;
609 65:547-52.
- 610 6. Lee JH, Kaminski N, Dolganov G, Grunig G, Koth L, Solomon C, et al. Interleukin-13
611 induces dramatically different transcriptional programs in three human airway cell types.
612 *Am J Respir Cell Mol Biol* 2001; 25:474-85.
- 613 7. Tliba O, Deshpande D, Chen H, Van Besien C, Kannan M, Panettieri RA, Jr., et al. IL-13
614 enhances agonist-evoked calcium signals and contractile responses in airway smooth
615 muscle. *Br J Pharmacol* 2003; 140:1159-62.
- 616 8. Amrani Y, Panettieri RA, Jr., Frossard N, Bronner C. Activation of the TNF alpha-p55
617 receptor induces myocyte proliferation and modulates agonist-evoked calcium transients
618 in cultured human tracheal smooth muscle cells. *Am J Respir Cell Mol Biol* 1996; 15:55-
619 63.
- 620 9. Hunter I. Tumor Necrosis Factor-alpha -Induced Activation of RhoA in Airway Smooth
621 Muscle Cells: Role in the Ca²⁺ Sensitization of Myosin Light Chain²⁰ Phosphorylation.
622 *Molecular Pharmacology* 2003; 63:714-21.

- 623 10. Chang Y, Al-Alwan L, Risse PA, Roussel L, Rousseau S, Halayko AJ, et al. TH17
624 cytokines induce human airway smooth muscle cell migration. *J Allergy Clin Immunol*
625 2011; 127:1046-53.e1-2.
- 626 11. Kudo M, Melton AC, Chen C, Engler MB, Huang KE, Ren X, et al. IL-17A produced by
627 alphabeta T cells drives airway hyper-responsiveness in mice and enhances mouse and
628 human airway smooth muscle contraction. *Nat Med* 2012; 18:547-54.
- 629 12. Wechsler ME, Ford LB, Maspero JF, Pavord ID, Papi A, Bourdin A, et al. Long-term
630 safety and efficacy of dupilumab in patients with moderate-to-severe asthma
631 (TRAVERSE): an open-label extension study. *Lancet Respir Med* 2022; 10:11-25.
- 632 13. Wenzel S, Ford L, Pearlman D, Spector S, Sher L, Skobieranda F, et al. Dupilumab in
633 persistent asthma with elevated eosinophil levels. *N Engl J Med* 2013; 368:2455-66.
- 634 14. Kirstein F, Horsnell WG, Kuperman DA, Huang X, Erle DJ, Lopata AL, et al. Expression
635 of IL-4 receptor alpha on smooth muscle cells is not necessary for development of
636 experimental allergic asthma. *J Allergy Clin Immunol* 2010; 126:347-54.
- 637 15. Perkins C, Yanase N, Smulian G, Gildea L, Orekov T, Potter C, et al. Selective
638 stimulation of IL-4 receptor on smooth muscle induces airway hyperresponsiveness in
639 mice. *J Exp Med* 2011; 208:853-67.
- 640 16. Doherty TA, Soroosh P, Khorram N, Fukuyama S, Rosenthal P, Cho JY, et al. The tumor
641 necrosis factor family member LIGHT is a target for asthmatic airway remodeling. *Nat*
642 *Med* 2011; 17:596-603.
- 643 17. Hastie AT, Moore WC, Meyers DA, Vestal PL, Li H, Peters SP, et al. Analyses of asthma
644 severity phenotypes and inflammatory proteins in subjects stratified by sputum
645 granulocytes. *J Allergy Clin Immunol* 2010; 125:1028-36.
- 646 18. Frossing L, Silberbrandt A, Von Bulow A, Kjaersgaard Klein D, Ross Christensen M,
647 Backer V, et al. Airway gene expression identifies subtypes of type 2 inflammation in
648 severe asthma. *Clin Exp Allergy* 2021; 52:59-69.

- 649 19. Hirano T, Matsunaga K, Oishi K, Doi K, Harada M, Suizu J, et al. Abundant TNF-LIGHT
650 expression in the airways of patients with asthma with persistent airflow limitation:
651 Association with nitrative and inflammatory profiles. *Respir Investig* 2021; 59:651-60.
- 652 20. da Silva Antunes R, Madge L, Soroosh P, Tocker J, Croft M. The TNF Family Molecules
653 LIGHT and Lymphotoxin alphabeta Induce a Distinct Steroid-Resistant Inflammatory
654 Phenotype in Human Lung Epithelial Cells. *J Immunol* 2015; 195:2429-41.
- 655 21. da Silva Antunes R, Mehta AK, Madge L, Tocker J, Croft M. TNFSF14 (LIGHT) Exhibits
656 Inflammatory Activities in Lung Fibroblasts Complementary to IL-13 and TGF-beta. *Front*
657 *Immunol* 2018; 9:576.
- 658 22. Manresa MC, Chiang AWT, Kurten RC, Dohil R, Brickner H, Dohil L, et al. Increased
659 Production of LIGHT by T Cells in Eosinophilic Esophagitis Promotes Differentiation of
660 Esophageal Fibroblasts Toward an Inflammatory Phenotype. *Gastroenterology* 2020.
- 661 23. Herro R, Shui JW, Zahner S, Sidler D, Kawakami Y, Kawakami T, et al. LIGHT-HVEM
662 signaling in keratinocytes controls development of dermatitis. *J Exp Med* 2018; 215:415-
663 22.
- 664 24. Herro R, Da Silva Antunes R, Aguilera AR, Tamada K, Croft M. Tumor necrosis factor
665 superfamily 14 (LIGHT) controls thymic stromal lymphopoietin to drive pulmonary
666 fibrosis. *J Allergy Clin Immunol* 2015; 136:757-68.
- 667 25. Xin HB, Deng KY, Rishniw M, Ji G, Kotlikoff MI. Smooth muscle expression of Cre
668 recombinase and eGFP in transgenic mice. *Physiol Genomics* 2002; 10:211-5.
- 669 26. Seo GY, Shui JW, Takahashi D, Song C, Wang Q, Kim K, et al. LIGHT-HVEM Signaling
670 in Innate Lymphoid Cell Subsets Protects Against Enteric Bacterial Infection. *Cell Host*
671 *Microbe* 2018; 24:249-60.e4.
- 672 27. Wang Y, Koroleva EP, Kruglov AA, Kuprash DV, Nedospasov SA, Fu YX, et al.
673 Lymphotoxin beta receptor signaling in intestinal epithelial cells orchestrates innate
674 immune responses against mucosal bacterial infection. *Immunity* 2010; 32:403-13.

- 675 28. Pham AK, Miller M, Rosenthal P, Das S, Weng N, Jang S, et al. ORMDL3 expression in
676 ASM regulates hypertrophy, hyperplasia via TPM1 and TPM4, and contractility. JCI
677 Insight 2021; 6.
- 678 29. Fong V, Hsu A, Wu E, Looney AP, Ganesan P, Ren X, et al. Arhgef12 drives IL17A-
679 induced airway contractility and airway hyperresponsiveness in mice. JCI Insight 2018;
680 3.
- 681 30. Himes BE, Koziol-White C, Johnson M, Nikolos C, Jester W, Klanderman B, et al.
682 Vitamin D Modulates Expression of the Airway Smooth Muscle Transcriptome in Fatal
683 Asthma. PLoS One 2015; 10:e0134057.
- 684 31. Sasse SK, Kadiyala V, Danhorn T, Panettieri RA, Jr., Phang TL, Gerber AN.
685 Glucocorticoid Receptor CHIP-Seq Identifies PLCD1 as a KLF15 Target that Represses
686 Airway Smooth Muscle Hypertrophy. Am J Respir Cell Mol Biol 2017; 57:226-37.
- 687 32. Tsukui T, Sun KH, Wetter JB, Wilson-Kanamori JR, Hazelwood LA, Henderson NC, et
688 al. Collagen-producing lung cell atlas identifies multiple subsets with distinct localization
689 and relevance to fibrosis. Nat Commun 2020; 11:1920.
- 690 33. Zepp JA, Zacharias WJ, Frank DB, Cavanaugh CA, Zhou S, Morley MP, et al. Distinct
691 Mesenchymal Lineages and Niches Promote Epithelial Self-Renewal and
692 Myofibrogenesis in the Lung. Cell 2017; 170:1134-48.e10.
- 693 34. Kumar A, D'Souza SS, Moskvina OV, Toh H, Wang B, Zhang J, et al. Specification and
694 Diversification of Pericytes and Smooth Muscle Cells from Mesenchymoangioblasts. Cell
695 Rep 2017; 19:1902-16.
- 696 35. Bara I, Ozier A, Tunon de Lara JM, Marthan R, Berger P. Pathophysiology of bronchial
697 smooth muscle remodelling in asthma. Eur Respir J 2010; 36:1174-84.
- 698 36. Brightbill HD, Suto E, Blaquiére N, Ramamoorthi N, Sujatha-Bhaskar S, Gogol EB, et al.
699 NF-kappaB inducing kinase is a therapeutic target for systemic lupus erythematosus.
700 Nat Commun 2018; 9:179.

- 701 37. Sakai H, Suto W, Kai Y, Chiba Y. Mechanisms underlying the pathogenesis of hyper-
702 contractility of bronchial smooth muscle in allergic asthma. *J Smooth Muscle Res* 2017;
703 53:37-47.
- 704 38. Andre-Gregoire G, Dilasser F, Chesne J, Braza F, Magnan A, Loirand G, et al. Targeting
705 of Rac1 prevents bronchoconstriction and airway hyperresponsiveness. *J Allergy Clin*
706 *Immunol* 2018; 142:824-33 e3.
- 707 39. Tong L, Tergaonkar V. Rho protein GTPases and their interactions with NFkappaB:
708 crossroads of inflammation and matrix biology. *Biosci Rep* 2014; 34.
- 709 40. Benayoun L, Druilhe A, Dombret MC, Aubier M, Pretolani M. Airway structural alterations
710 selectively associated with severe asthma. *Am J Respir Crit Care Med* 2003; 167:1360-
711 8.
- 712 41. Lauzon AM, Martin JG. Airway hyperresponsiveness; smooth muscle as the principal
713 actor. *F1000Res* 2016; 5.
- 714 42. Chiba Y, Ueno A, Shinozaki K, Takeyama H, Nakazawa S, Sakai H, et al. Involvement of
715 RhoA-mediated Ca²⁺ sensitization in antigen-induced bronchial smooth muscle
716 hyperresponsiveness in mice. *Respir Res* 2005; 6:4.
- 717 43. Eum SY, Maghni K, Tolloczko B, Eidelman DH, Martin JG. IL-13 may mediate allergen-
718 induced hyperresponsiveness independently of IL-5 or eotaxin by effects on airway
719 smooth muscle. *Am J Physiol Lung Cell Mol Physiol* 2005; 288:L576-84.
- 720 44. Moynihan B, Tolloczko B, Michoud MC, Tamaoka M, Ferraro P, Martin JG. MAP kinases
721 mediate interleukin-13 effects on calcium signaling in human airway smooth muscle
722 cells. *Am J Physiol Lung Cell Mol Physiol* 2008; 295:L171-7.
- 723 45. Farghaly HS, Blagbrough IS, Medina-Tato DA, Watson ML. Interleukin 13 increases
724 contractility of murine tracheal smooth muscle by a phosphoinositide 3-kinase
725 p110delta-dependent mechanism. *Mol Pharmacol* 2008; 73:1530-7.

- 726 46. Chiba Y, Nakazawa S, Todoroki M, Shinozaki K, Sakai H, Misawa M. Interleukin-13
727 augments bronchial smooth muscle contractility with an up-regulation of RhoA protein.
728 Am J Respir Cell Mol Biol 2009; 40:159-67.
- 729 47. Chang Y, Al-Alwan L, Risse PA, Halayko AJ, Martin JG, Baglole CJ, et al. Th17-
730 associated cytokines promote human airway smooth muscle cell proliferation. FASEB J
731 2012; 26:5152-60.
- 732 48. Nakajima M, Kawaguchi M, Ota K, Fujita J, Matsukura S, Huang SK, et al. IL-17F
733 induces IL-6 via TAK1-NFκB pathway in airway smooth muscle cells. Immun Inflamm
734 Dis 2017; 5:124-31.
- 735 49. Bulek K, Chen X, Parron V, Sundaram A, Herjan T, Ouyang S, et al. IL-17A Recruits
736 Rab35 to IL-17R to Mediate PKCα-Dependent Stress Fiber Formation and Airway
737 Smooth Muscle Contractility. J Immunol 2019; 202:1540-8.
- 738 50. McKnight CG, Potter C, Finkelman FD. IL-4Rα expression by airway epithelium and
739 smooth muscle accounts for nearly all airway hyperresponsiveness in murine allergic
740 airway disease. Mucosal Immunol 2020; 13:283-92.

741

742

743 **Figure Legends**

744 **Figure 1. $LT\beta R$ and HVEM are expressed by human healthy and asthmatic airway smooth**
 745 **muscle cells.** (A) Expression of transcripts of the receptors for LIGHT, TNF, IL-13/IL-4, and IL-
 746 17 from published RNA-seq data of human healthy and asthmatic ASM (GSE119578/9;
 747 GSE58434; GSE94335). (B) Flow analysis of $LT\beta R$ and HVEM expression on healthy and asthma
 748 donor-derived ASM.

749

750 **Figure 2. ASM-specific $LT\beta R$ -deficient mice exhibit reduced ASM mass and AHR in**
 751 **allergen-induced experimental severe asthma.** (A) HVEM and $LT\beta R$ expression on ASM
 752 (GFP⁺) from smMHC^{Cre}(eGFP), smMHC^{Cre}HVEM^{fl/fl} or smMHC^{Cre} $LT\beta R$ ^{fl/fl} mice. Data from 3
 753 experiments. (B-G) smMHC^{Cre}, smMHC^{Cre}HVEM^{fl/fl}, or smMHC^{Cre} $LT\beta R$ ^{fl/fl} mice were given
 754 intranasal challenges of HDM extract over 6 weeks (n = 4-6/group). (B) Confocal analysis of lung
 755 bronchi (scale 20 μ m). F-actin (Phalloidin, yellow), alpha smooth muscle actin (red), DAPI (blue).
 756 Data representative of 3 experiments. (C) Quantitation of ASM volume based on phalloidin
 757 staining around the bronchi from (B) (n = 6-9/group, 10-15 tertiary bronchi per mouse). Data
 758 representative of 3 experiments. (D) Airway resistance (AHR) after methacholine challenge,
 759 measured by Flexivent (n = 5-8/group). Data representative of two experiments. *P < 0.05,
 760 smMHC^{Cre} vs. $LT\beta R$ ^{fl/fl}. (E) Flow quantitation of total lung tissue smooth muscle cells (ASM). Data
 761 points, individual mice. (F) Flow quantitation of total lung inflammatory/immune cells. Data points,
 762 individual mice. (G) Representative H&E stained lung sections (scale 100 μ m). n =4-6 mice/group.
 763 Data representative of 3 experiments. Means \pm SEM. *P < 0.05, **P < 0.01.

764

765 **Figure 3. LIGHT- $LT\beta R$ signals increase airway smooth muscle mass and induce AHR in**
 766 **mice.** Mice received intratracheal recombinant LIGHT or PBS over 3 days. (A-B) Confocal
 767 microscopy of lung bronchial sections for expression of F-actin (Phalloidin, yellow) and α -smooth

768 muscle actin (red). (A) Representative images of bronchi (scale 20 μm). (B) Imaris 3D imaging
769 analysis quantification of ASM volume (phalloidin) around individual bronchi (n = 4-5 mice/group,
770 10-15 tertiary bronchi per mouse). Data means \pm SEM and representative of 3 experiments. *P <
771 0.05, **P < 0.01. (C) Airway resistance (AHR) after methacholine challenge, measured by
772 Flexivent (n = 4 mice/group). *P < 0.05, smMHC^{Cre} vs. LT β R^{fl/fl}. Data means \pm SEM and
773 representative of 2 experiments.

774

775 **Figure 4. LIGHT induces human ASM proliferation and contractile activity.** (A) HVEM and
776 LT β R expression on human ASM assessed by flow after stimulation with LIGHT for 24 or 48hr.
777 Similar data in 3 experiments. (B) Images of ASM in collagen 3D gels. Left: Bright field, Right:
778 Phalloidin (red), DAPI (blue). (C) ASM collagen gel contraction at 24-72hr after stimulation with
779 LIGHT. Data combined means from triplicates from 3 experiments. (D) Percentages of BrdU⁺
780 ASM stimulated with LIGHT for 48hr. Cells either first incubated in serum free media for 16 hours
781 for proliferative ASM, or for 7 days for contractile ASM. Data means of triplicates and
782 representative of 3 experiments. (E) ASM volume after stimulation with LIGHT, measured by
783 confocal microscopy. 300-400 ASM, in two replicate experiments were analyzed. Data means \pm
784 SEM. *P < 0.05, **P < 0.01, ***P < 0.001, ****P < 0.0001.

785

786 **Figure 5. LIGHT induces actin polymerization and migratory ability in human ASM.** (A) RNA-
787 seq analysis of contractile molecules in human ASM treated with LIGHT. Log2 fold change after
788 4hr compared to PBS treated cells. (B) GSEA of cell structure-related genes from RNA-seq of
789 ASM stimulated with LIGHT compared to PBS for 4hr. (C) Confocal images of ASM treated with
790 LIGHT for 6hr and stained with Phalloidin (red), Vinculin (green), DAPI (blue). Graphs show
791 volume of F-actin (phalloidin) and focal adhesions (vinculin) normalized to individual cell sizes
792 (scale 15 μm). 300-400 ASM, in two replicate experiments were analyzed. (D) Images of wounded
793 monolayers of ASM stimulated with LIGHT for 12hr; left, fluorescence intensity of F-actin shown

794 (yellow to red); right, remaining wound highlighted in yellow outline. Percentage of wound area
795 remaining after LIGHT stimulation compared to PBS (scale 200 μm). Data combined from 3
796 independent experiments. Data means \pm SEM. * $P < 0.05$, ** $P < 0.01$, *** $P < 0.001$.

797

798 **Figure 6. LIGHT-dependent non-canonical NF- κ B signaling induces actin polymerization**
799 **and ASM contractility.** (A) Activation of canonical NF- κ B (pp65) and non-canonical NF- κ B
800 (processing of p100 to p52) assessed in human ASM stimulated with LIGHT over 120 mins or
801 24hr. Data representative of 3 experiments. (B) Confocal analysis of ASM treated with LIGHT with
802 or without NIK-SMI, an inhibitor of non-canonical NF- κ B. Volume of phalloidin and vinculin
803 normalized to cell size from triplicates (scale 10 μm). 300-400 ASM, in two replicate experiments
804 were analyzed. (C) Gel contraction assay of LIGHT-stimulated ASM with or without inhibitors of
805 canonical (BAY11-7082) and non-canonical (NIK-SMI) NF- κ B. Percentage gel contraction
806 compared to PBS in triplicates. Data representative of 2 experiments. Data means \pm SEM. ** $P <$
807 0.01, *** $P < 0.001$, **** $P < 0.0001$.

808

809 **Figure 7. LIGHT induces non-canonical NF- κ B-dependent activation of Rac1/PAK1 and**
810 **phosphorylation of MLC in ASM.** (A-C) pMLC2 (A), pMYPT and pPAK1 (B), and active Rac1-
811 GTP immunoprecipitated with PAK1 (C) in human ASM stimulated with LIGHT for the indicated
812 times. (D-E) Processing of p52, and pPAK1 (D) and pMLC2 (E) in ASM stimulated with LIGHT for
813 12hr, with or without inhibitors of canonical (BAY) and non-canonical NF- κ B (NIK-SMI). (F) Active
814 Rac1-GTP immunoprecipitated with PAK1 in ASM stimulated with LIGHT for 4hr with or without
815 NIK-SMI. All data in A-F representative of 3 experiments. (G) Gel contraction of ASM stimulated
816 with LIGHT, with or without an inhibitor of Rac1. Percentage gel contraction compared to PBS in
817 triplicates. (H) Confocal analysis of ASM treated with LIGHT with or without a Rac1 inhibitor.
818 Volume of phalloidin and vinculin normalized to cell size from triplicates (scale 10 μm). 300-400

819 ASM, in two replicate experiments were analyzed. Data representative of 2 experiments. Data
820 means \pm SEM. **P < 0.01, ***P < 0.001, ****P < 0.0001.

Journal Pre-proof

Figure 1

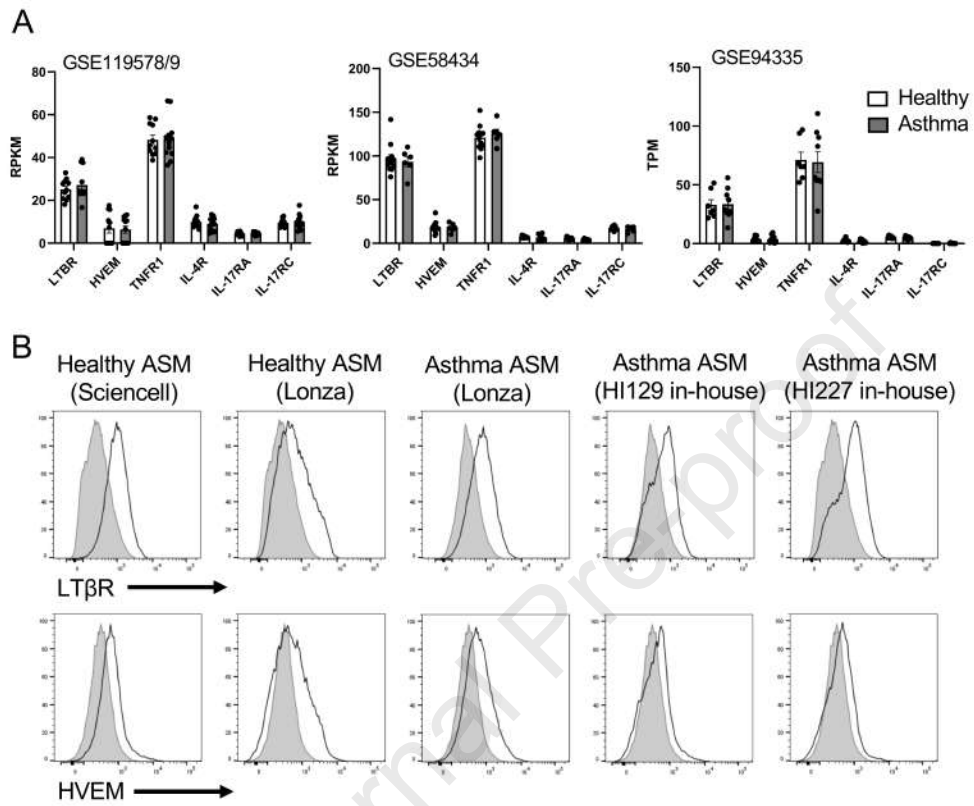


Figure 2

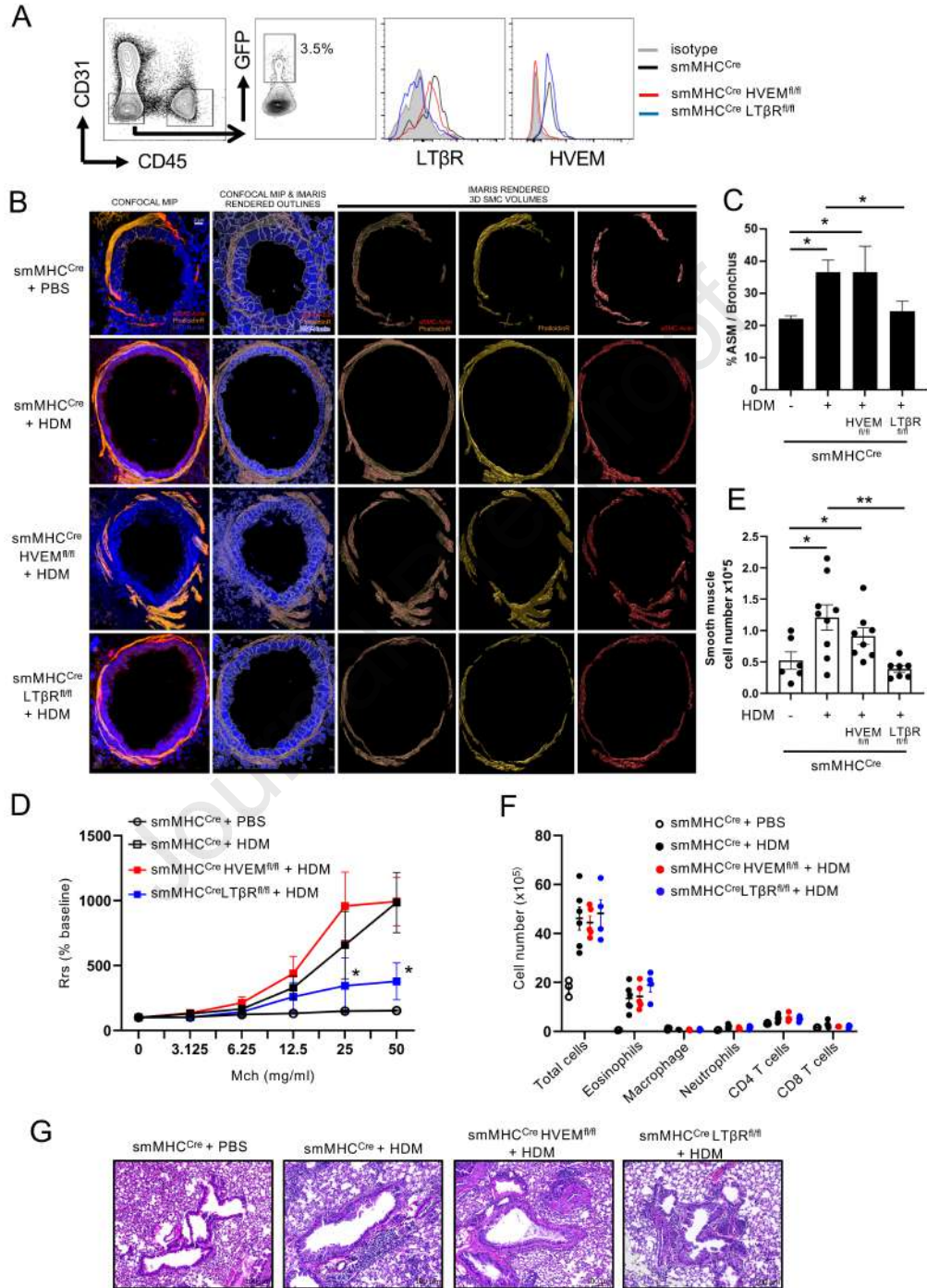


Figure 3

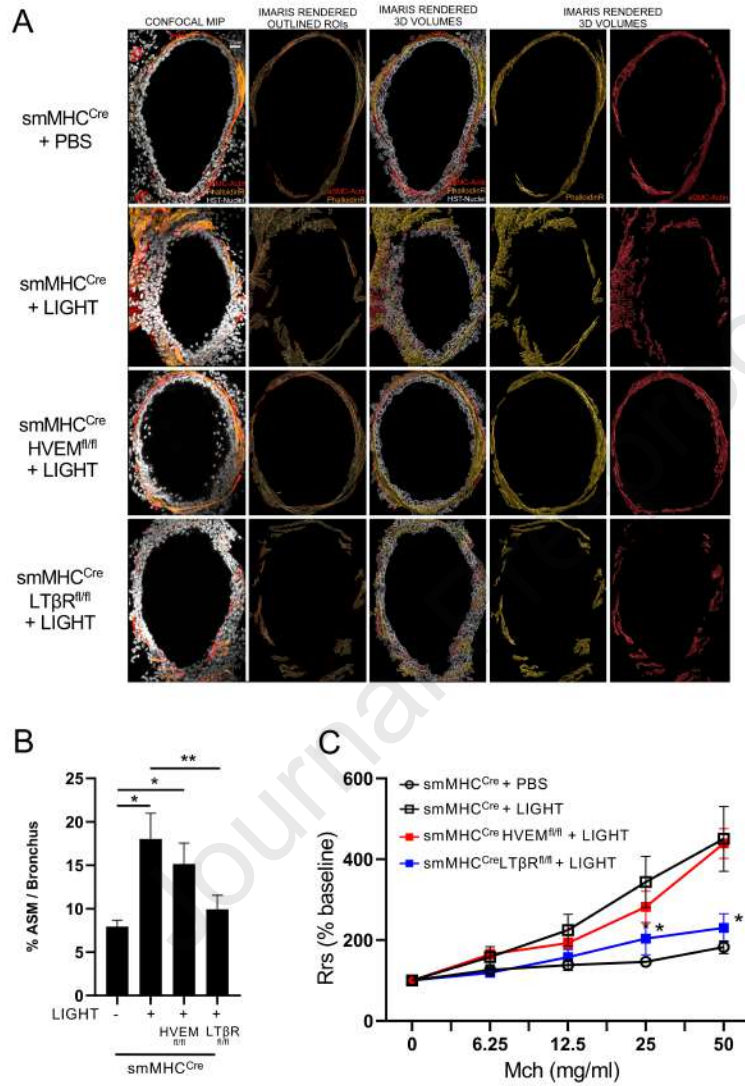


Figure 4

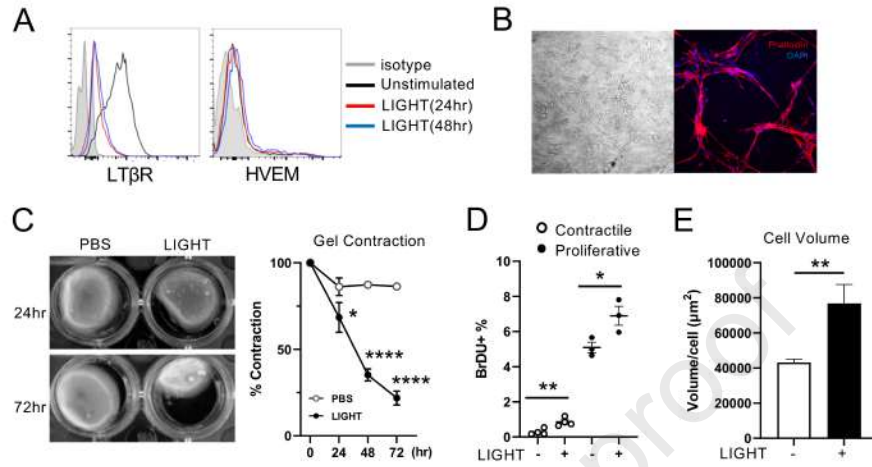


Figure 5

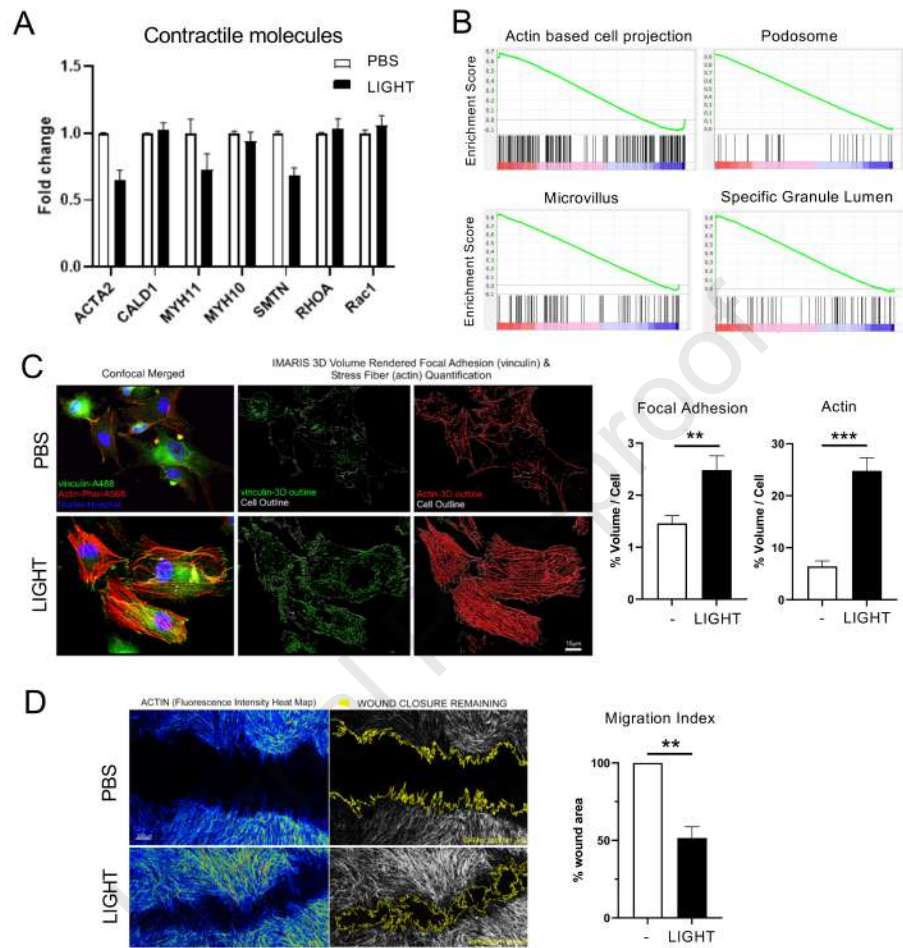


Figure 6

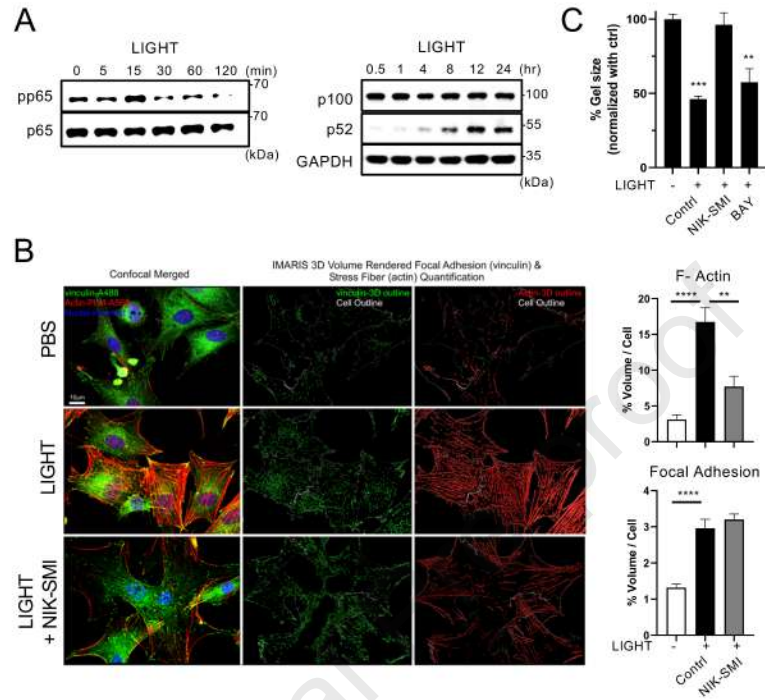


Figure 7

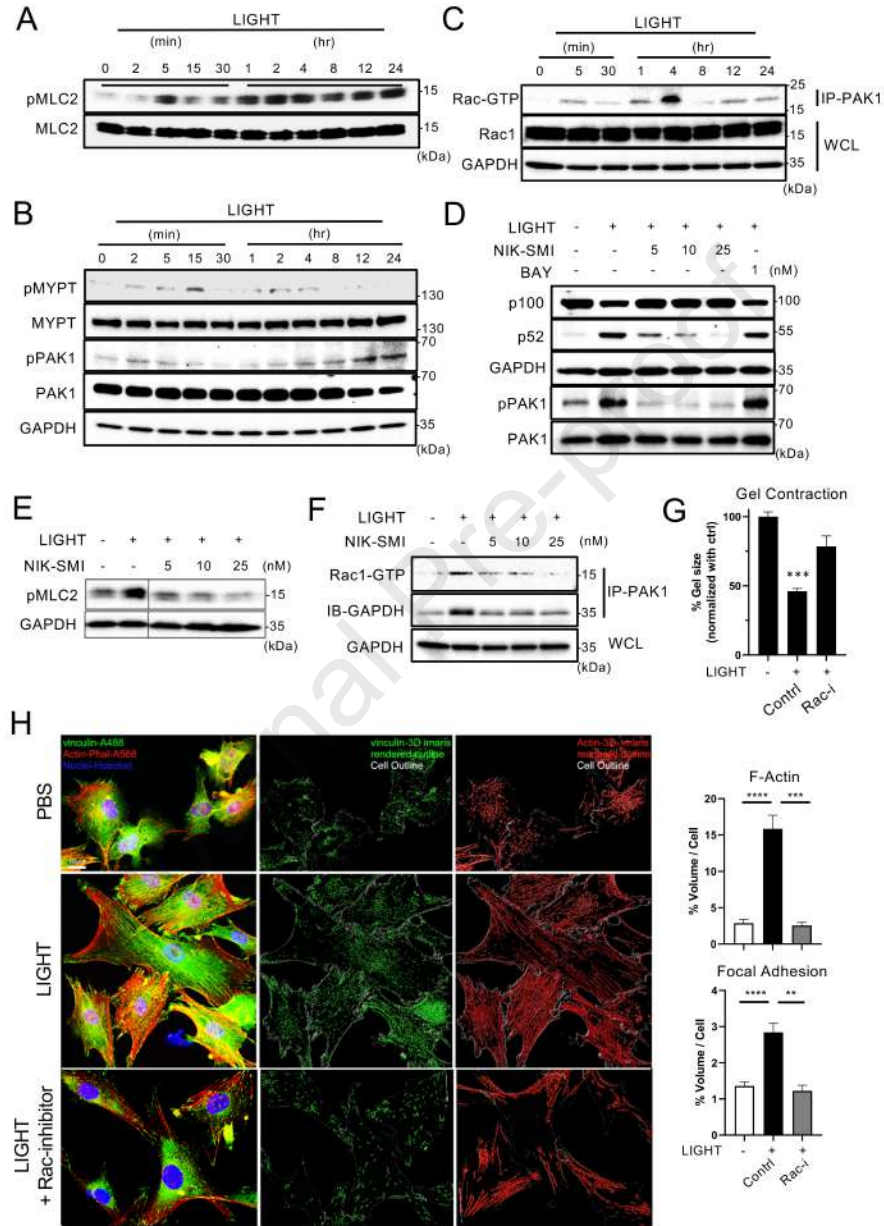


Figure E1

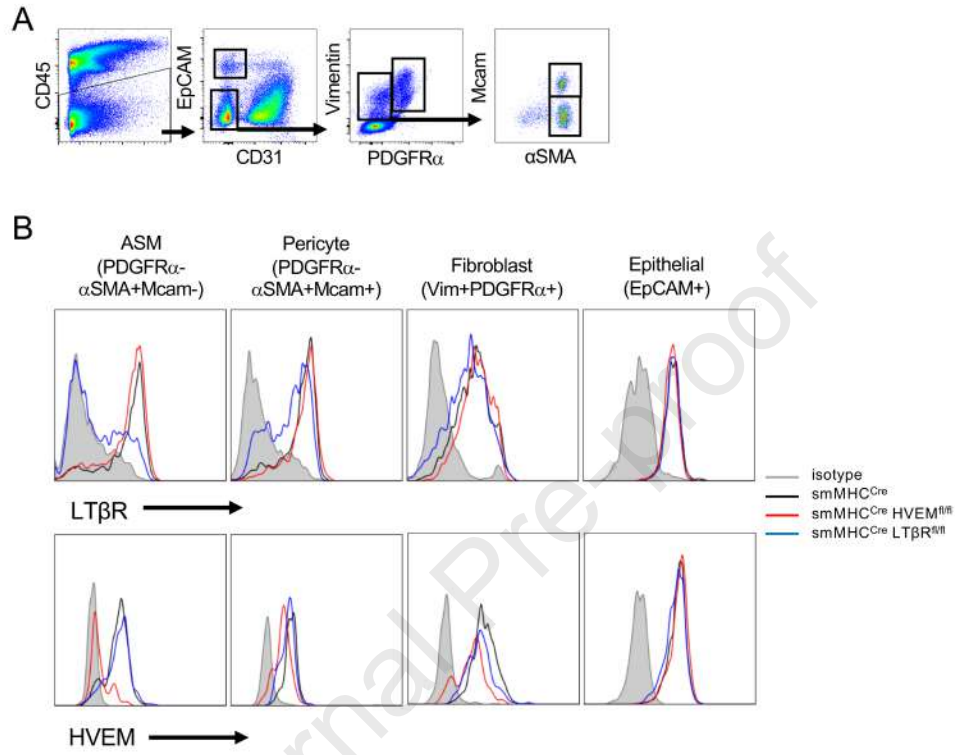


Figure E2

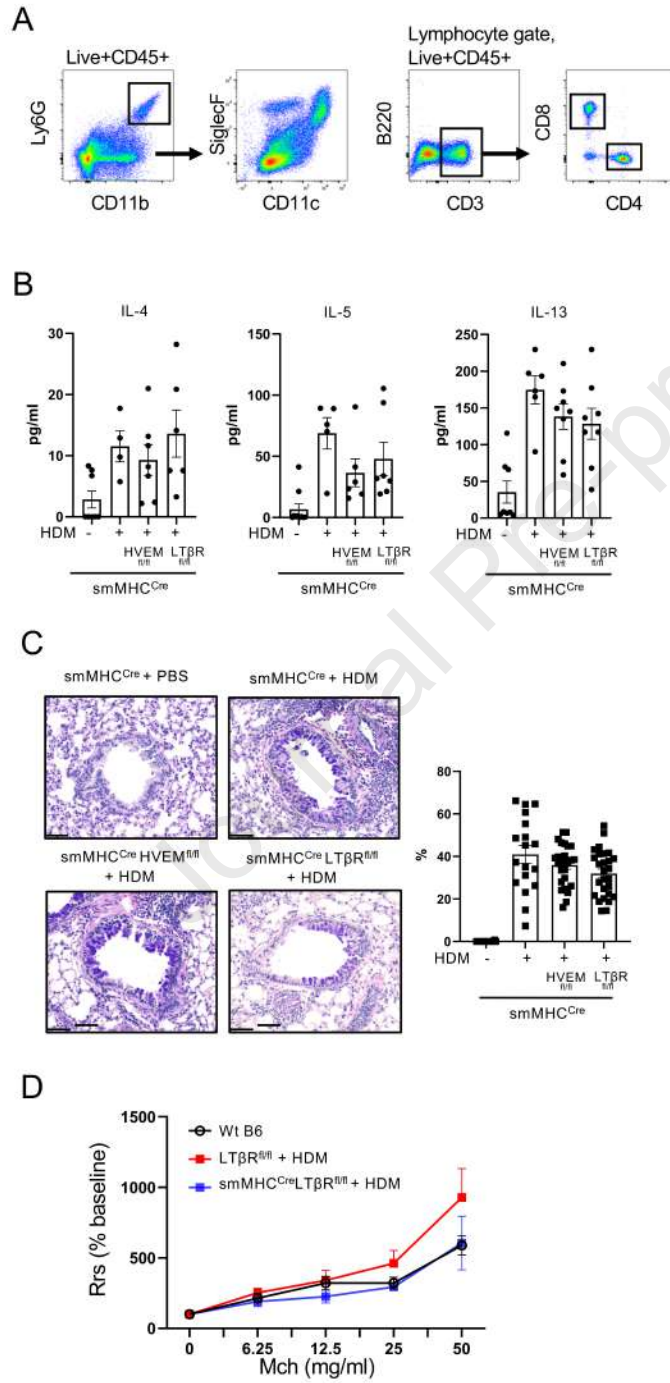


Figure E3

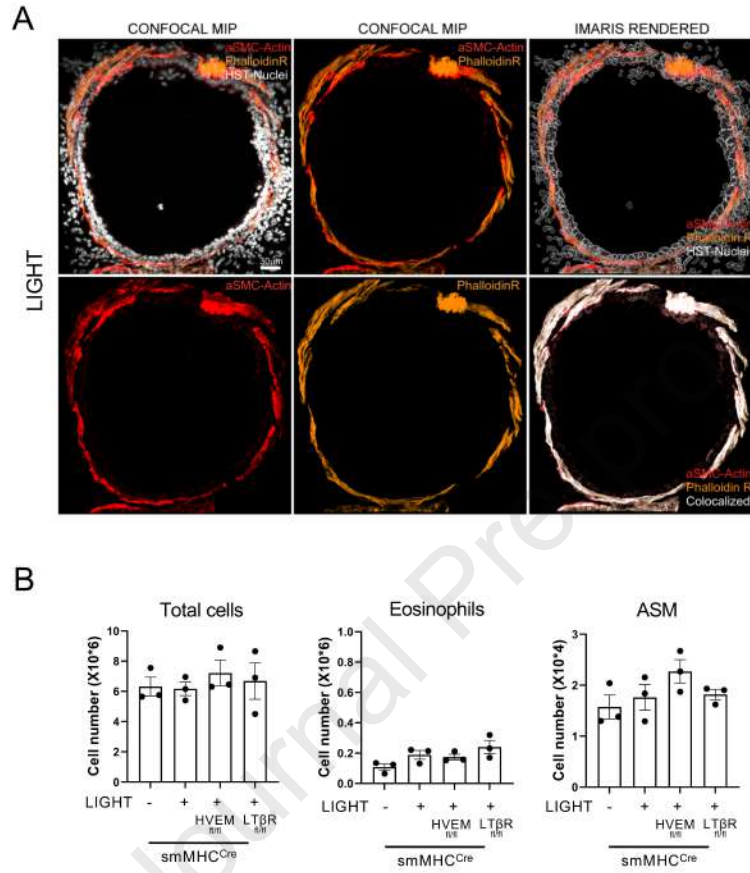


Figure E4

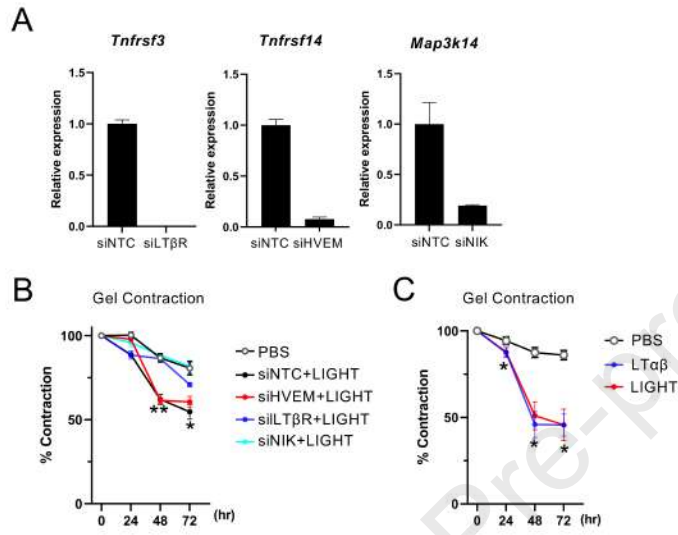
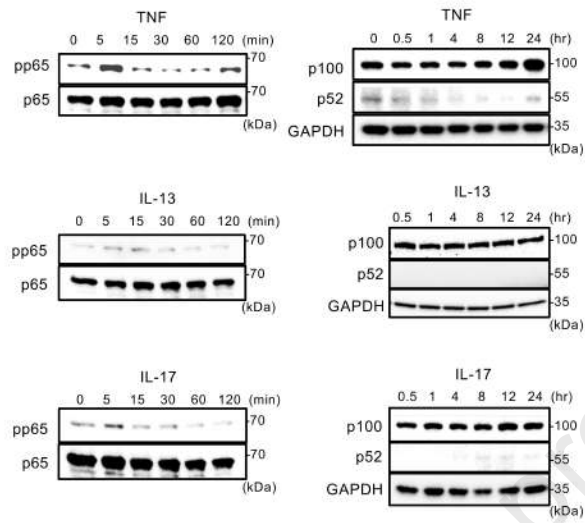


Figure E5



1 **Supplementary Figure Legends**

2

3 **Figure E1. Flow cytometry analysis of lung structural cells.** (A) Flow gating of epithelial cells
 4 (CD45⁺EpCAM⁺CD31⁻), fibroblasts (CD45⁻EpCAM⁻CD31⁻Vimentin^{hi}PDGFR α ⁺), pericytes (CD45⁻
 5 EpCAM⁻CD31⁻Vimentin^{med}PDGFR α ⁻ α SMA⁺Mcam⁺), and ASM (CD45⁻EpCAM⁻CD31⁻
 6 Vimentin^{med}PDGFR α ⁻ α SMA⁺Mcam⁻) in mouse lungs. (B) Expression of HVEM and LT β R on gated
 7 lung structural cells from smMHC^{Cre}, smMHC^{Cre}HVEM^{fl/fl}, or smMHC^{Cre}LT β R^{fl/fl} mice.

8

9 **Figure E2. Analysis of inflammatory features in allergen-induced lungs, and AHR in acute**
 10 **lung inflammation.** (A) Flow gating of CD45⁺ lung immune cells; Neutrophils (CD11b⁺Ly6G⁺),
 11 Eosinophils (CD11b⁺Ly6G⁻CD11c^{lo}SiglecF⁺), Alveolar macrophages (CD11b⁺Ly6G⁻
 12 CD11c⁺SiglecF⁺), CD4⁺ T cells (CD3⁺CD4⁺CD8⁻) and CD8⁺ T cells (CD3⁺CD4⁻CD8⁺). (B) IL-4, IL-
 13 5 and IL-13 production in BAL fluid of smMHC^{Cre}, smMHC^{Cre}HVEM^{fl/fl}, or smMHC^{Cre}LT β R^{fl/fl} mice
 14 challenged chronically with HDM over 6 weeks (n = 6-8/group). (C) Representative PAS stained
 15 lung sections (scale 100 μ m) and percentages of PAS-positive bronchial epithelial cells. n =4-5
 16 mice/group, 5 bronchi per mouse. Data representative of 3 experiments. (D) Airway resistance
 17 (AHR) after methacholine challenge, measured by Flexivent (n = 4-5 mice/group), in mice acutely
 18 challenged with HDM over 14 days. Data means \pm SEM.

19

20 **Figure E3. Bronchial smooth muscle and other cellular changes in mice injected with**
 21 **LIGHT.** (A) Confocal images of lung bronchi from mice treated with LIGHT and stained with
 22 Phalloidin (orange) and α -smooth muscle actin (red), scale 30 μ m. (B) smMHC^{Cre},
 23 smMHC^{Cre}HVEM^{fl/fl}, or smMHC^{Cre}LT β R^{fl/fl} mice were treated intratracheally with LIGHT or PBS,
 24 and numbers of total cells, eosinophils, or ASM in lung tissues were analyzed by flow cytometry.

25

26 **Figure E4. Involvement of $LT\beta R$ and NIK in ASM contractility.** (A) mRNA expression of Tnfrsf3
27 ($LT\beta R$), Tnfrsf14 (HVEM) and Map3k14 (NIK) in ASM after siRNA targeting. (B) Gel contraction
28 of ASM with siRNA knockdown after stimulation with LIGHT. (C) Gel contraction of ASM
29 stimulated with LIGHT or $LT\alpha\beta$. Means \pm SEM from triplicate cultures. Data means \pm SEM and
30 representative of 2 experiments. *P < 0.05, **P < 0.01.

31

32 **Figure E5. TNF, IL-13, and IL-17 activation of canonical or non-canonical NF- κ B in ASM.**

33 Activation of canonical NF- κ B (pp65, left) and non-canonical NF- κ B (processing of p100 to p52,
34 right) assessed in human ASM stimulated for various times with TNF, IL-13 or IL-17.